Selected Cosmic-Ray Orbits in the Earth's Magnetic Field*†

F. S. JORY‡

The Enrico Fermi Institute for Nuclear Studies and Department of Physics, University of Chicago, Chicago, Illinois

(Received August 24, 1955)

A set of 663 charged-particle orbits in the earth's dipole magnetic field has been obtained by integration, using the AVIDAC computer of the Argonne National Laboratory. The orbits integrated were selected according to their usefulness in the analysis of cosmic-ray intensity increases associated with solar flares. The calculation of intensity increases for different locations on the earth is discussed using the orbit results.

I. INTRODUCTION

LARGE and moderate sized solar flares are known to be associated with an increase in the counting rate of suitably placed cosmic-ray detectors on the earth.[1,2] One theory to explain the flare-effect assumes that positively charged particles of cosmic-ray energies are produced at or very near the sun. They travel away from the sun within a wide cone filling practically one hemisphere of solid angle.[3] There is some scattering of the particles due to magnetic fields between the sun and the earth.[4] However, it seems reasonable to a sume that when the particles are first deflected in the earth's magnetic field, their velocity vectors all fall uniformly within a given cone in velocity space, the axis of the cone being defined by the sun-earth line. The solid angle of the cone opening is the apparent source solid

FIG. 1. Impact directions: Initial tangent directions with respect to an observer of an outgoing negatively charged particle orbit.

angle and the geomagnetic latitude of the sun is the source latitude. The influence of the earth's magnetic field is, of course, to deflect the particles so that some will arrive at the earth in preferred regions called impact zones and the others will be deflected away. It has been shown[1] that experimental results are approximately in agreement with the above theory in so far as we have information about the intensities to be expected in the impact zones. (Of special interest are the cosmic-ray intensity increases observed outside of estimated impact zones by stations at high latitudes.[2,5,6]) Detailed discussions of the flare effect by several investigators have indicated the need for calculating more orbits of charged particles in the earth's magnetic field in order to define the impact zone intensities for various source latitudes and source solid angles. Therefore this paper reports the integration of 663 cosmic-ray orbits in the earth's dipole magnetic field. The orbits were selected with an application to the flare-effect in mind. For the purpose of illustration,
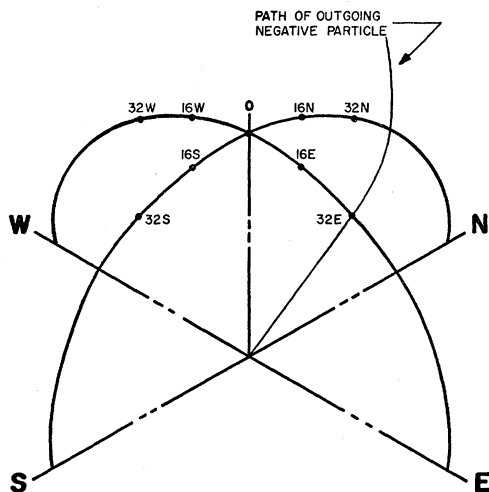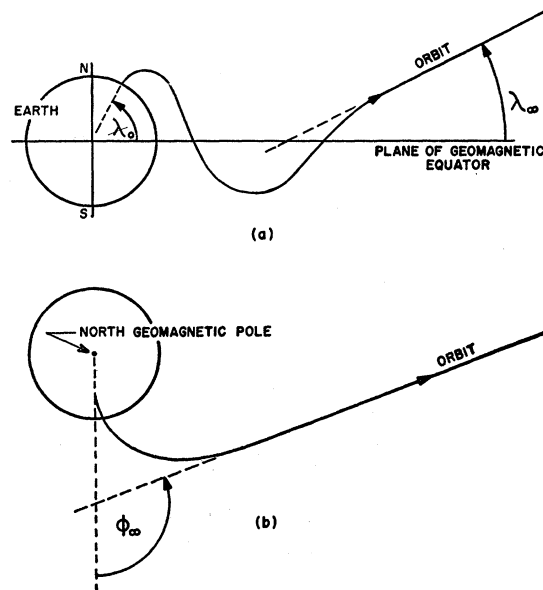

FIG. 2. (a) Asymptotic latitude λ_∞ and (b) asymptotic longitude φ_∞ of an outgoing negatively charged particle orbit. The impact latitude is λ_0. This figure is taken from reference 1.

[1] J. Firor, Phys. Rev. **94**, 1017 (1954).
[2] Forbush, Stinchcomb, and Schein, Phys. Rev. **79**, 501 (1950).
[3] Simpson, Firor, and Treiman, Phys. Rev. **95**, 1015 (1954).
[4] S. B. Treiman, Phys. Rev. **94**, 1029 (1954).
[5] D. C. Rose, Can. J. Phys. **29**, 227 (1951).
[6] J. W. Graham and S. E. Forbush, Phys. Rev. **98**, 1348 (1955).

TABLE I. Grouping of orbits by impact zones.

Number of orbits per zone	Impact zone	
444	0900	
174	0300	
39	2000	Background zone
6	1300	

the orbit information is used to compute impact zone intensities during a hypothetical solar flare.

II. ORBITS OF COSMIC-RAY PARTICLES

For the application of orbit knowledge to the flare-effect, we are not interested in the detailed path of the orbit, but only in where and how the orbit intersects the earth and what is the orbit direction outside the earth's magnetic field. In the literature there is considerable orbit information, obtained both from integration (Stoermer,[7] Schlüter,[8] Dwight,[9] Firor,[1] and others) and from model experiments (Malmfors,[10] Brunberg and Dattner[11]). There are two ways to obtain an orbit by integration: start at infinity and integrate toward the earth, or start at the earth and integrate outward to infinity. Orbits started at infinity arrive at the earth with a random direction of impact, and therefore tend to arrive at the earth with large zenith angles. Near vertical impact, however, is by far the

TABLE II. Values of λ_∞ and φ_∞ in degrees for orbits with 0° impact latitude.

N (Bv)	A (Stoermer)	32E	16E	0	Impact direction 16W	32W	32N	16N
26.0	0.66	0.0 136.3	0.0 98.1	0.0 72.7	0.0 52.7	0.0 36.1	9.5 84.1	6.4 75.6
24.4	0.64	0.0 151.6	0.0 106.1	0.0 78.6	0.0 57.8	0.0 40.8	6.6 90.3	5.0 81.6
22.9	0.62		0.0 116.0	0.0 85.6	0.0 63.5	0.0 46.0	3.1 97.7	3.5 88.7
21.5	0.60		0.0 128.7	0.0 93.9	0.0 70.2	0.0 52.0	−0.9 106.7	1.6 97.1
20.4	0.585		0.0 141.5	0.0 101.3	0.0 76.0	0.0 57.0	−4.2 115.2	0.0 104.8
19.4	0.57		0.0 159.4	0.0 110.2	0.0 82.6	0.0 62.7	−7.7 126.0	−1.8 114.0
18.4	0.555			0.0 121.3	0.0 90.3	0.0 69.1	−10.9 140.7	−3.7 125.6

TABLE III. Values of λ_∞ and φ_∞ in degrees for orbits with 10° impact latitude.

N (Bv)	A (Stoermer)	32E	16E	0	Impact direction 16W	32W	32N	16N	16S	32S
26.0	0.66	−8.0 130.4	−6.3 94.5	−1.6 70.3	3.2 51.4	7.5 35.7	3.7 86.9	3.6 76.3	−8.7 69.7	−14.8 74.7
24.4	0.64	−6.5 143.5	−7.2 101.9	−2.9 75.9	2.0 56.2	6.5 40.2	−0.4 92.6	1.0 81.9	−8.8 75.3	−13.5 80.6
22.9	0.62	−2.8 162.4	−7.9 111.0	−4.2 82.3	0.6 61.6	5.3 45.2	−4.9 99.7	−1.9 88.4	−8.7 81.9	−11.7 87.4
21.5	0.60		−8.1 122.5	−5.6 90.0	−0.9 67.9	3.9 50.9	−9.7 108.7	−5.0 96.4	−8.4 89.7	−9.4 95.3
20.4	0.585		−7.3 133.7	−6.6 96.9	−2.2 73.2	2.6 55.7	−13.2 117.4	−7.3 103.7	−7.9 96.5	−7.2 102.4
19.4	0.57		−5.2 148.4	−7.5 105.1	−3.6 79.4	1.2 61.0	−16.1 129.0	−9.7 112.6	−7.1 104.6	−4.5 110.8
18.4	0.555			−8.0 115.1	−5.0 86.5	−0.4 67.0	−16.7 145.0	−11.4 123.9	−5.8 114.4	−1.0 121.1

[7] C. Stoermer, Astrophys. Norv. **1**, 1 (1936).
[8] A. Schlüter, Z. Naturforsch. **6a**, 613 (1951), and Mexico City Cosmic-Ray Conference (1955).
[9] K. Dwight, Phys. Rev. **78**, 40 (1950).
[10] K. G. Malmfors, Arkiv. Mat. Astron. Fysik. **32A**, No. 8 (1945).
[11] E. Brunberg, Tellus **5**, 135 (1953) and E. Brunberg and A. Dattner, Tellus **5**, 269 (1953).

TABLE IV. Values of λ_∞ and φ_∞ in degrees for orbits with 20° impact latitude.

N (Bv)	A (Stoermer)	Impact direction 32E	16E	0	16W	32W	32N	16N	16S	32S
21.5	0.60	−8.2	−15.5	−8.4	0.6	9.1	−14.8	−8.6	−11.8	−16.1
		151.0	106.0	79.6	61.5	48.0	100.8	88.1	75.5	76.4
20.1	0.58	3.6	−15.8	−11.1	−2.5	6.1	−19.8	−12.8	−13.0	−15.6
		174.1	117.0	86.9	67.4	53.4	110.6	95.9	82.8	83.7
18.7	0.56	11.8	−13.9	−13.7	−6.0	2.4	−22.9	−16.7	−13.8	−14.5
		240.1	131.5	96.0	74.3	59.6	124.6	106.2	91.6	92.4
17.4	0.54		−6.9	−15.5	−9.7	−1.8	−20.1	−18.9	−13.9	−12.4
			151.6	107.9	82.8	66.8	144.8	120.4	102.6	103.1
16.1	0.52		9.9	−14.9	−13.3	−6.5	−2.1	−16.3	−12.2	−8.4
			187.3	124.0	93.7	75.6	173.5	140.6	116.9	116.6
15.5	0.51		11.1				16.8			
			239.8				200.8			
14.9	0.50			−8.5	−15.8	−11.5		−0.6	−6.7	−1.3
				146.9	108.5	86.7		171.7	136.6	135.3
14.0	0.485			4.9	−15.3	−14.9		12.7	2.5	7.3
				175.1	123.7	97.7		245.7	159.1	157.2
13.6	0.477			14.6						
				206.3						
13.2	0.470			−12.3	−9.8	−16.9			13.2	11.9
				333.7	144.6	112.4			210.4	206.4
12.4	0.455				6.8	−14.5				
					179.3	132.8				

TABLE V. Values of λ_∞ and φ_∞ in degrees for orbits with 30° impact latitude.

N (Bv)	A (Stoermer)	Impact direction 32E	16E	0	16W	32W	32N	16N	16S	32S
18.0	0.55	−11.7	−22.6	−15.1	−4.2	5.9	−27.0	−19.3	−14.8	−16.9
		139.8	102.7	78.9	64.5	55.4	103.6	89.2	71.6	67.2
16.1	0.52	10.5	−20.3	−20.4	−11.8	−2.7	−27.3	−24.7	−18.4	−18.3
		165.7	120.5	91.3	73.7	63.5	123.0	104.0	83.0	78.0
14.9	0.50	18.8	−12.9	−22.2	−17.0	−9.3	−18.6	−24.5	−19.8	−18.5
		214.0	135.6	102.9	82.1	70.2	138.3	118.3	93.1	87.1
14.3	0.49	1.0								
		334.5								
13.7	0.48		2.6	−20.5	−21.3	−16.1	0.4	−12.1	−19.2	−17.3
			155.2	117.9	93.4	79.1	154.2	135.5	106.0	98.5
12.6	0.46		20.7	−11.5	−22.6	−22.0	23.4	2.0	−14.4	−13.5
			200.0	137.0	109.1	91.6	182.6	156.4	122.5	112.8
12.1	0.45		−20.1							
			295.2							
11.6	0.44			9.7	−16.1	−23.7	−22.7	21.0	−1.5	−4.7
				164.7	130.0	109.8	268.6	208.9	144.8	131.9
11.1	0.432							−21.1		
								295.5		
10.7	0.423			−2.8	1.3	−16.5			16.9	9.0
				247.3	153.3	130.2			181.3	157.6
10.3	0.415								9.0	
									227.9	
9.9	0.407				19.7	3.6				5.6
					207.1	154.4				229.2
9.18	0.392					16.5				
						216.1				

TABLE VI. Values of λ_∞ and φ_∞ in degrees for orbits with 40° impact latitude.

N (Bv)	A (Stoermer)	Impact direction								
		32E	16E	0	16W	32W	32N	16N	16S	32S
14.9	0.50	−25.6	−24.8	−16.8	−7.3	0.4	−29.0	−22.8	−12.9	−11.1
		96.8	79.5	66.9	59.3	55.3	82.9	75.2	58.8	51.3
13.2	0.47	−21.0	−25.6	−22.3	−15.8	−10.3	−29.1	−27.0	−17.9	−14.6
		102.9	88.3	74.6	65.6	60.5	88.8	83.1	66.3	58.7
11.6	0.44	−15.0	−22.7	−25.0	−22.9	−20.3	−24.7	−26.4	−21.7	−18.1
		107.7	97.8	85.0	74.7	68.0	91.7	92.2	76.5	68.5
10.3	0.416	−10.2	−17.7	−23.5	−25.5	−25.6	−19.9	−22.3	−22.5	−20.1
		111.7	105.1	94.8	84.6	76.8	91.5	98.3	87.1	79.1
9.26	0.394	−6.4	−12.1	−18.9	−23.5	−25.8	−15.7	−17.1	−20.2	−20.1
		117.4	112.0	103.8	94.6	86.2	92.0	102.4	98.8	91.8
8.34	0.374	−2.9	−6.6	−12.8	−18.4	−21.9	−13.1	−12.5	−14.8	−16.8
		127.6	120.4	112.2	103.3	93.8	97.0	106.8	111.0	106.6
7.57	0.356	2.7	−1.1	−6.5	−12.4	−16.7	−12.4	−9.0	−6.9	−9.0
		146.5	132.7	121.7	111.2	99.7	109.6	114.4	124.3	123.4
6.88	0.340	13.1	6.3	−0.1	−6.7	−12.2	−9.5	−5.4	2.9	3.8
		190.8	153.7	135.1	120.5	106.3	132.8	128.3	141.1	144.3
6.34	0.326		13.0	7.9	−1.0	−8.4	9.8	2.5	13.5	16.7
			204.6	157.1	134.0	116.4	175.8	153.0	168.6	181.8
6.12	0.320						15.2			
							192.3			
5.85	0.313			10.0	7.7	−3.2		7.8	−12.5	
				218.4	158.7	134.1		233.7	268.9	
5.60	0.306				13.6	2.6				
					188.0	150.5				

TABLE VII. Values of λ_∞ and φ_∞ in degrees for orbits with 50° impact latitude.

N (Bv)	A (Stoermer)	Impact direction								
		32E	16E	0	16W	32W	32N	16N	16S	32S
14.9	0.50	−14.5	−7.4	1.4	9.7	15.5	−10.4	−4.5	5.9	9.0
		48.2	46.6	45.1	44.5	44.8	51.2	49.9	38.4	31.2
12.1	0.45	−11.7	−10.1	−5.9	−1.5	1.3	−10.4	−9.9	−1.1	3.4
		47.7	47.2	46.2	45.3	44.3	46.3	48.0	42.3	37.9
10.0	0.41	−8.2	−9.6	−9.1	−7.7	−6.4	−4.1	−9.1	−6.5	−3.4
		50.6	49.2	47.6	45.7	43.0	44.9	47.2	46.3	44.4
8.61	0.38	−8.5	−9.2	−9.6	−9.0	−7.2	−0.6	−6.5	−10.0	−9.6
		57.4	53.4	50.3	46.9	42.6	50.2	49.4	50.5	50.3
7.32	0.35	−15.4	−11.5	−10.4	−8.5	−4.8	−7.5	−7.2	−13.3	−15.6
		69.9	62.2	56.3	51.0	45.8	62.8	57.4	56.9	57.6
6.12	0.32	−23.5	−20.1	−16.0	−12.0	−8.2	−23.1	−17.4	−17.2	−19.1
		89.3	77.8	68.8	61.9	57.5	80.3	73.0	67.4	67.1
5.38	0.30	−20.2	−22.5	−21.3	−19.0	−17.8	−23.4	−23.6	−20.2	−19.7
		100.6	92.1	82.1	74.5	70.5	89.1	87.7	78.4	75.7
4.74	0.282	−15.0	−18.3	−21.3	−22.6	−23.5	−18.1	−20.5	−20.7	−19.7
		104.8	102.7	96.2	89.7	85.0	88.9	97.5	91.7	87.2
4.20	0.265	−11.8	−13.1	−15.8	−18.4	−19.8	−17.0	−15.7	−16.7	−17.5
		116.1	111.5	107.2	101.5	93.6	100.5	102.6	106.7	104.5
3.72	0.250	1.9	−6.5	−10.1	−13.3	−15.9	−8.8	−12.2	−8.9	−8.2
		149.2	130.7	120.4	111.3	101.4	134.2	120.1	123.4	125.8
3.50	0.242	18.0								
		192.7								
3.35	0.237	−17.0	14.9	2.4	−5.8	−10.9	15.9	7.9	4.2	7.4
		275.9	175.8	147.9	133.0	125.2	168.0	158.8	147.9	150.8
3.15	0.230		−16.4					15.6		
			298.4					208.2		
3.01	0.225			−9.5	17.5	15.6	14.7	14.6	9.1	12.9
				257.2	189.8	172.0	186.3	361.6	221.8	208.5

TABLE VIII. Values of λ_∞ and φ_∞ in degrees for orbits with 60° impact latitude.

N (Bv)	A (Stoermer)	32E	16E	0	16W	32W	32N	16N	16S	32S
						Impact direction				
14.9	0.50	11.8	16.9	23.6	29.7	33.5	13.9	18.4	28.1	31.8
		27.8	30.8	33.5	36.3	39.0	37.5	37.4	27.2	20.2
10.5	0.42	19.0	18.1	18.5	19.5	20.4	22.2	18.4	20.5	22.4
		31.1	30.3	30.7	30.6	28.9	29.6	30.2	30.3	29.8
7.73	0.36	9.4	14.2	16.9	19.6	23.8	19.6	19.7	14.0	11.1
		42.4	38.3	34.3	30.8	27.7	43.5	37.4	33.0	31.8
5.74	0.31	−2.0	1.1	5.9	10.1	11.9	0.5	2.9	7.3	8.4
		40.6	41.4	40.8	40.1	40.2	41.5	43.0	37.3	33.9
4.37	0.27	−1.2	0.2	0.4	1.2	4.0	4.4	2.9	−0.3	−1.0
		48.0	44.3	42.3	40.4	37.5	46.9	42.7	42.5	42.7
3.72	0.25	−11.8	−7.0	−3.2	0.0	2.5	−9.3	−4.4	−4.4	−5.7
		53.2	51.0	47.8	45.3	44.8	51.8	50.6	46.2	44.7
3.15	0.23	−9.8	−11.5	−10.8	−9.8	−9.3	−5.5	−10.7	−9.2	−7.7
		54.1	53.6	53.0	51.7	49.4	51.3	52.4	51.6	50.2
2.63	0.21	−19.2	−15.6	−13.1	−11.1	−9.4	−17.8	−14.2	−14.3	−15.5
		67.3	63.4	59.5	56.6	55.6	63.4	62.1	59.2	58.9
2.20	0.192	−18.7	−18.1	−18.7	−18.6	−16.3	−18.7	−16.9	−18.6	−18.3
		75.3	71.6	70.2	68.0	63.6	73.2	68.8	69.8	69.4
1.88	0.177	−19.4	−21.0	−21.1	−21.0	−21.6	−18.8	−21.2	−20.5	−19.9
		87.7	88.5	85.0	81.9	80.2	81.5	85.7	83.1	81.3
1.45	0.156	−10.8	−12.2	−13.4	−15.0	−16.6	−12.5	−14.4	−14.0	−14.4
		123.8	117.0	115.2	112.2	104.2	120.1	112.1	114.4	113.6
1.27	0.147	1.9	3.1	−1.2	−4.4	−5.9	−1.2	−1.0	−2.0	−2.7
		144.3	144.4	138.8	134.0	128.6	141.3	136.9	136.6	134.5
1.14	0.139	13.5	15.6	15.0	11.3	12.4	14.6	17.2	15.6	16.1
		206.5	203.4	176.5	164.4	163.9	177.1	187.7	177.8	179.2

most efficient trajectory for secondary cosmic-ray production in the atmosphere. Hence there is need for information about near-vertical orbits. In order to specify the angle of impact with the earth, the integration of an orbit was thus begun at the earth. The problem of "What is the orbit of a positively charged particle arriving at the earth?" was replaced by the equivalent problem, "What is the orbit of a negatively charged particle being shot away from the earth?" The geomagnetic latitude of an observer on the earth will be called the impact latitude λ_0. Ten-degree intervals of impact latitude were selected, 0°, 10°, 20°, etc. The impact longitude was set equal to zero. The direction an observer must look in order to observe an incoming positive particle will be referred to as the "impact direction." It is the tanget direction, with respect to the observer, of an outgoing negative particle orbit. Impact directions were selected 32, 16, or 0 degrees from the vertical, successively toward geomagnetic north, east, south, and west (Fig. 1). The integration proceeded from the earth outward until the asymptotic latitude and asymptotic longitude could be computed (Fig. 2). The magnetic rigidity $N = pc/Ze$ of an orbit

was selected by choosing a value for A, the earth's radius in Stoermer units.

It is obvious from the differential equations of motion that the orbit of a negative particle of magnetic rigidity N, shot away from the earth at impact latitude λ_0 with given impact direction, will have a unique asymptotic latitude λ_∞ and unique asymptotic longitude φ_∞, provided it can escape from the dipole field. As mentioned above, for discussion of the flare effect it is useful to know λ_∞ and φ_∞ as a function of λ_0, N, and impact direction. One point of view is to assume λ_0 and the impact direction are held constant and N is allowed to vary. For extremely high rigidity the orbit will essentially be a straight line. As rigidity decreases, the variation of λ_∞ and φ_∞ is known down to moderate rigidities, from the model experiments of Malmfors[10] and Brunberg.[11] Their experiments give information about orbits that are bent around the earth approximately from 0 to 90 degrees in longitude, i.e., orbits belonging to the first impact zone centered about 0900 local time. For the present orbit program, values of A were selected corresponding to lower rigidities than those of the model experiments, but higher than the

cutoff rigidity for the particular λ_0 and impact direction. Many different values of A are necessary so that adjacent values of rigidity result in neighboring values of λ_∞, φ_∞. In this manner the model experiment results were extended to other impact zones than the 0900 impact zone. Near the cutoff rigidity, of course, the orbits take on a complicated behavior, the radius vector from dipole to particle alternately decreasing and increasing.[7] Orbits with a decreasing radius vector were not included in this program.

A set of 663 orbits was obtained by integration, using the AVIDAC at the Argonne National Laboratory, Lemont, Illinois. Again it should be emphasized that we were not interested in the detailed path of an orbit but solely in the magnetic rigidity, impact latitude, and impact direction and the resulting asymptotic latitude and asymptotic longitude. Since only one intermediate point of the orbit was printed out, there resulted a considerable saving of machine time. If an orbit went monotonically outward, the integration was continued to a distance of ten Stoermers, at which point the asymptotic latitude and asymptotic longitude were computed. The error introduced by stopping at ten Stoermers was estimated to be at most $\frac{1}{4}$ degree. The error in latitude is generally less than the error in longitude. By comparison, the error due to taking a

TABLE IX. Values of λ_∞ and φ_∞ in degrees for orbits with 70° impact latitude.

N (Bv)	A (Stoermer)	Impact direction				
		32E	0	32W	32N	32S
14.9	0.50	37.7	46.1	52.9	37.8	54.1
		17.2	27.4	38.1	32.0	12.4
10.5	0.42	44.4	44.0	45.1	47.8	44.7
		26.2	24.0	21.2	24.5	24.2
7.73	0.36	33.1	42.4	50.5	42.8	37.2
		33.2	27.4	21.6	40.1	19.7
5.74	0.31	31.8	35.2	38.4	32.5	39.3
		24.2	28.6	31.2	28.2	22.7
4.37	0.27	27.9	33.3	38.3	33.9	29.8
		33.2	28.4	24.9	36.3	25.8
3.72	0.25	24.4	29.5	33.1	25.9	30.8
		28.1	30.6	32.0	31.0	24.6
3.15	0.23	26.0	26.6	28.9	30.0	26.3
		32.8	29.5	26.7	33.6	29.7
2.63	0.21	20.2	23.2	25.0	21.9	24.5
		30.1	32.2	32.8	31.0	28.1
2.20	0.192	15.4	20.4	24.4	17.4	18.4
		34.5	32.5	32.0	35.6	30.6
1.88	0.177	14.9	16.1	19.0	16.7	16.0
		36.4	33.6	31.4	37.4	33.7
1.45	0.156	8.0	11.1	12.2	10.7	10.3
		36.6	36.8	37.1	36.2	34.8
1.27	0.147	4.5	8.0	10.6	6.4	6.7
		39.4	37.9	37.9	38.4	37.4

TABLE X. Values of λ_∞ and φ_∞ in degrees for orbits with 80° impact latitude.

N (Bv)	A (Stoermer)	Impact direction				
		32E	0	32W	32N	32S
14.9	0.50	61.3	68.2	72.4	60.3	75.0
		7.2	24.4	49.0	32.8	−2.2
10.5	0.42	67.2	67.5	68.3	71.0	66.0
		27.7	21.2	14.3	23.8	20.8
7.73	0.36	57.0	66.5	75.0	65.6	62.1
		29.1	24.5	16.2	47.5	6.6
5.74	0.31	61.8	63.2	64.6	61.1	66.7
		16.9	23.8	29.2	24.0	18.1
4.37	0.27	56.1	62.4	68.1	61.9	59.6
		27.3	24.0	20.5	37.5	14.0
3.72	0.25	58.2	60.4	62.2	58.2	63.1
		18.8	24.5	28.9	25.2	17.7
3.15	0.23	56.7	59.7	62.8	61.5	57.3
		28.5	23.3	18.6	32.3	20.2
2.63	0.21	57.5	57.7	58.2	57.9	59.6
		21.8	24.4	25.3	23.4	21.9
2.20	0.192	53.2	56.7	59.2	54.3	57.1
		22.1	24.7	27.4	27.2	18.3
1.88	0.177	51.7	55.3	58.5	54.4	53.8
		25.6	24.1	23.9	26.2	20.2
1.45	0.156	52.6	52.6	52.5	53.9	53.6
		24.5	25.1	24.2	25.2	23.7
1.27	0.147	50.8	51.6	51.8	51.7	52.5
		23.4	25.1	26.0	24.5	22.5

step of finite size in the integration procedure was found to be 0.001 percent. A test for systematic errors was made by comparing a machine-computed orbit with a hand-computed orbit. The agreement was within the estimated errors.

Previous work on the solar flare effect has pointed out that a solar cosmic-ray source in the geomagnetic equatorial plane would give increases in zones, the first two being centered on 0900 and 0300 local time.[1] As the sun moves northward off the geomagnetic equatorial plane, these two zones move apart in the nothern hemisphere and merge in the southern hemisphere. Theoretically, there is a series of such zones, the third and fourth being centered on 2000 and 1300 local time for an equatorial source. It has been pointed out[1] that after the first and second zones, the following zones do not have a very strong local time dependence and might well be grouped together into a background zone. Inasmuch as a given orbit can be said to belong to one zone or another, the 663 orbits of the program were grouped into zones as shown in Table I.

III. IMPACT ZONE INTENSITIES

In order to estimate the intensities expected in impact zones during a solar flare, we note that according to Liouville's theorem if a plane wave of particles, all
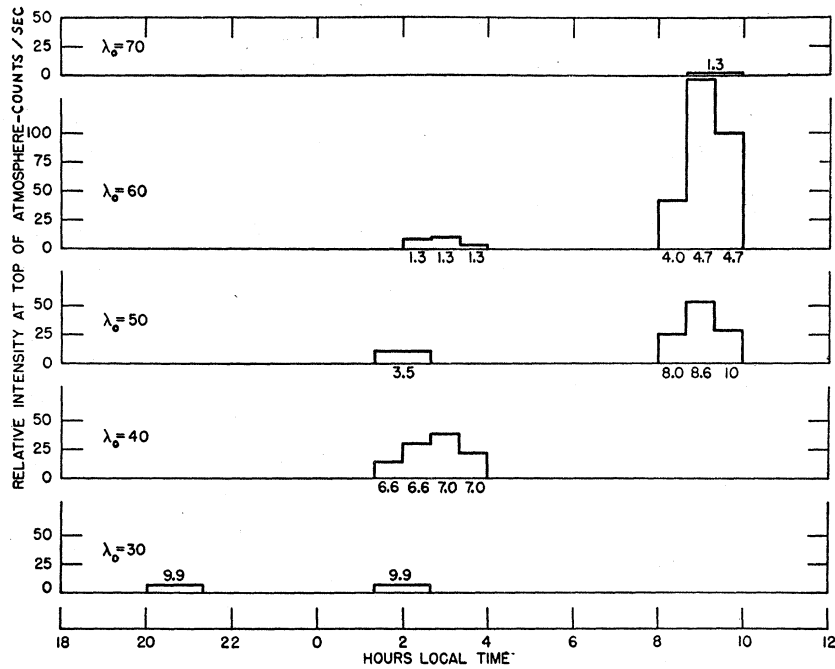
FIG. 3. Counting rates which would be expected during a hypothetical solar flare for an ideal detector at the top of the atmosphere. The same detector would have a counting rate of 100 counts per second outside the earth's magnetic field. The assumed source latitude, source solid angle, and rigidity spectrum are noted in the text. The numbers above or below the histogram values refer to the mean rigidity in Bv arriving at the top of the atmosphere.

with the same rigidity, comes toward the earth, an observer at the top of the atmosphere looking in a certain direction will either see the full intensity, or nothing at all. Thus if there is a spectrum of rigidities and a finite source solid angle, the problem is what fraction of the solid angle at the top of the atmosphere is allowed.[12]

Assume that a detector is omnidirectional and one hundred percent efficient for all cosmic ray rigidities. Assume it were to be placed outside the earth's magnetic field, and that the normal cosmic-ray background were to be zero. Then the count rate of this detector during a solar flare would be the integral rigidity spectrum of solar flare particles times the solid angle of the source. On the other hand, if the same detector is placed at the top of the atmosphere at point P, the flare particles arriving at the detector will have suffered deflection in the earth's magnetic field. The count rate at P will be the differential rigidity spectrum $j(N)$ of solar-flare particles times the allowed solid angle $\Omega_P(N)$ integrated over rigidity. N_{min} and N_{max} are the minimum and maximum rigidity of the solar flare particle spectrum. $\Omega_P(N)$ depends implicitly on the latitude of P, the local time at P, the source latitude, and source solid angle.

$$I_P = \int_{N_{min}}^{N_{max}} j(N)\Omega_P(N)dN.$$

For a given rigidity, there are parts of an impact zone where the allowed solid angle at the top of the atmosphere is greater than the solid angle of the source. Physically this amounts to a focusing property of the earth's magnetic field with respect to cosmic-rays. i.e.,

a wide solid angle detector counts particles coming from a narrow solid angle outside the earth's magnetic field. There can also be defocusing. For example, when very close to the cutoff rigidity, the allowed solid angle at the earth is much less than the source solid angle. Some specific examples of focusing are considered by Åström.[13]

The AVIDAC results are listed in Tables II–X. The double entries in the tables signify that the upper number is λ_∞ in degrees, the lower number is φ_∞ in degrees. From the tables a hypothetical flare has been studied: sun in the geomagnetic equator, source solid angle ± 5 degrees extent in latitude, ± 10 degrees extent in longitude. It will be noted that a rectangular source was assumed for convenience. The source was assumed to emit a flat spectrum from 1 to 10 Bv, normalized so that the idealized detector has a count rate of 100 per second. For this source latitude and source solid angle, 47 orbits were found connecting points on the earth with the source. Some points on the earth had several orbits starting in different directions from the top of the atmosphere and connecting with the source. The allowed solid angle at a given location was taken to be proportional to the number of connecting orbits. This could introduce an error of possibly 20% in the intensity predicted at a given location. The integral I_P was approximated by a summation. The counting rates which would be expected for the idealized detector at the top of the atmosphere are given as a function of local time for different latitudes in Fig. 3. The mean rigidity (in Bv) arriving at the top of the atmosphere is also noted. It is clear that this distribution of intensity in the impact

[12] S. B. Treiman (private communication).

[13] E. Åström, Tellus (to be published).

zones depends on the particular choice of source latitude, source spectrum, and source solid angle.

There is the additional comment that at 50 degrees latitude, the 0900 impact zone receives higher rigidity particles, the 0300 impact zone lower rigidity particles, whereas at latitude 60 degrees, both the high and the low rigidity particles are received in the 0900 zone. This tendency for observers at middle latitudes to see monorigidity solar flare particles, and observers at higher latitudes (60 degrees) to see the integrated spectrum, is not too sensitive to source latitude and source solid angle.

Heavy Primary Cosmic Radiation at the Equator*

R. E. DANIELSON,† P. S. FREIER, J. E. NAUGLE, AND E. P. NEY
Department of Physics, University of Minnesota, Minneapolis, Minnesota
(Received April 16, 1956)

The zenith and azimuthal angular distribution of primary cosmic rays with charges ≥ 6 has been measured at the equator using oriented nuclear emulsions. The magnitude of the azimuthal asymmetry is consistent with an integral power law spectrum which falls off inversely as the 2.0 power of the total energy per nucleon. However, the maximum intensity comes from the southwest rather than the west. This is consistent with the recently proposed shift of the earth's effective magnetic field for cosmic rays.

The flux at the top of the atmosphere is 0.68 particle m^{-2} sec^{-1} $sterad^{-1}$ for CNOF (carbon, nitrogen, oxygen, fluorine) nuclei and 0.21 particle m^{-2} sec^{-1} $sterad^{-1}$ for nuclei with $Z \geq 10$.

INTRODUCTION

EARLY counter measurements[1] of east-west asymmetries have always resulted in asymmetries which are smaller than that predicted by geomagnetic theory, assuming that the incident flux is isotropic and that all the primary cosmic rays are positively charged. Part of this discrepancy is no doubt caused by nonprimary radiation[2] in the form of secondary particles, resulting from interactions with air nuclei, which enter the counter telescope from below. This effect would be especially large at large zenith angles, and this is where the discrepancy is the greatest. If one were to measure the asymmetries of heavy nuclei, however, one could be certain as to the primary character of the particles. Therefore an orienter was designed to orient horizontal nuclear emulsions with respect to the earth's magnetic field.

A second purpose of this experiment was to measure the primary flux of the heavy component at the equator. This flux measurement constitutes an important point on the integral energy spectrum for the heavies.

A knowledge of the analytic form of this integral energy spectrum is important since the exponent in the proper law (if one assumes that a power law of the total energy is the correct analytical form) appears to be larger for heavy primaries than for protons. This would be useful information concerning the acceleration mechanism and lifetime of the primary cosmic radiation.

The third purpose of this experiment was to resolve the charge spectrum as much as possible. This is of interest since the comparison of relative abundances of the elements in the primary cosmic radiation at various energies with the observed abundances in the universe is valuable information concerning the lifetime and sources of cosmic radiation. Any marked deviation of the abundances of the components of the cosmic rays from the observed abundances in the universe provides important data in devising an origin theory.

BALLOON FLIGHTS AND APPARATUS

Two balloon flights were flown as part of Project Churchy, a cosmic-ray expedition to the Galapagos Islands near the geographic equator. The time-altitude curve for Flight 2 is shown in Fig. 1. The flight record for Flight 1 is similar. The trajectory of the balloon was approximately straight from the launch point (geographic latitude 0°20'S; geographic longitude 90°20'W) to the splash point (1°20'S; 96°10'W).

[1] Winckler, Stix, Dwight, and Sabin, Phys. Rev. 79, 666 (1950).
[2] K. A. Anderson, Ph.D. thesis, University of Minnesota, 1955 (unpublished).